VNU Journal of Science: Mathematics – Physics, Vol. 37, No. 3 (2021) 109-118

VNU Journal of Science: Mathematics - Physics

Journal homepage: https://js.vnu.edu.vn/MaP

Original Article

Dynamic Analysis of Eccentrically Stiffened Sandwich Thick Plates with Auxetic Honeycomb Core and GPL-RC Face Layers under Blast Loading

Vu Dinh Quang[1,*]

VNU University of Engineering and Technology, 144 Xuan Thuy, Cau Giay, Hanoi, Vietnam

Received 19 June 2021
Revised 22 July 2021; Accepted 05 August 2021

Abstract: This study analyses eccentrically stiffened sandwich thick plates with the core layer made of negative poisson material. The analytical method based on the first order shear deformation theory (FSDT) is applied to analyse dynamic response and vibration of the plates. The numerical results of the study have been compared with other studies to evaluate the reliability of the calculation. The analysis results of the nonlinear dynamic response and the vibration show that the elastic foundation and the graphene volume ratio positively impact the behavior of the plates. On the other hand, imperfection and thermal environment have a negative effect on the behavior of sandwich plates. Research has also been performed to evaluate the effect of blast load, axial load and shape on the dynamic response of the plate.

Keywords: Sandwich plates, FSDT, auxetic, dynamic response, vibration, blast loads

1. Introduction

Composite materials have been applied widely in advanced industries in the world such as aviation, aerospace, ship building, machinery, construction, etc. because composite materials have got more unique advantages such as light weight, high modulus of elasticity, high heat-insulation, high sound isolation than conventional metals. Composite materials are combined from two substances with different properties, whereas homogeneous elasticity substances are attached together to improve mechanical behavior of materials. Recently, the sandwich structures have been studied by many scientists. Sandwich structures combined with new materials are a matter of great interest.

*Corresponding author.
Email address: quangvd2510@vnu.edu.vn

https//doi.org/ 10.25073/2588-1124/vnumap.4654

Recently, structures with layers of auxetic materials have received special attention. Nam et al. [1] investigated the behavior of the auxetic honeycomb sandwich plate using the finite element method based on higher-order shear deformation theory, the plate model has meshed with the polygon element. Sandwich plate with layer core made of auxetic 3D was studied by Chong Li et al., post-buckling behavior and vibration were examined [2,3]. Mohammad et al. [4] researched the dynamic response of the plate with two faces layer made of composite reinforced by carbon nanotubes. Research on the mechanics of plate structures with auxetic layers has been interested in recent years by other authors [5, 6].

Currently, FSDT has been commonly used to investigate sandwich plates. Thai et al. [7] investigated bending, buckling and free vibration of the functionally graded sandwich plate using an analytical method based on FSDT. Phuong et al. [8] examined buckling and vibration of sandwich plate with both homogeneous hardcore and softcore and functionally graded faces based on FSDT. Amir et al. [9] analyzed buckling of sandwich plate with flexoelectric face layers and carbon nanotubes reinforced composite core using FSDT. Duc et al. [10] investigated vibration and nonlinear dynamic response of FGM plate with top layer made of piezoelectric material.

The aim of this research is to analyze nonlinear dynamic response and vibration of eccentrically stiffened sandwich thick plates with auxetic honeycomb score and GPL-RC face layers based on the first order shear deformation theory. Using FSDT, this research considers the effect of geometric parameter, material properties, foundation parameter, mechanical and thermal loads on the dynamic response of the thick plate.

2. Analytical Solution

2.1. Model of Plates and Material Properties

This study considers plate models with two face layers made from graphene platelet reinforced composite (GPL) and an auxetic core layer.

The reaction–deflection relation is given by

$$q_e = K_W w - K_P \nabla^2 w \qquad (1)$$

with ∇ is Laplace operator, w is the deflection, K_W and K_P are Winkler foundation stiffness and shear layer stiffness of Pasternak foundation, respectively.

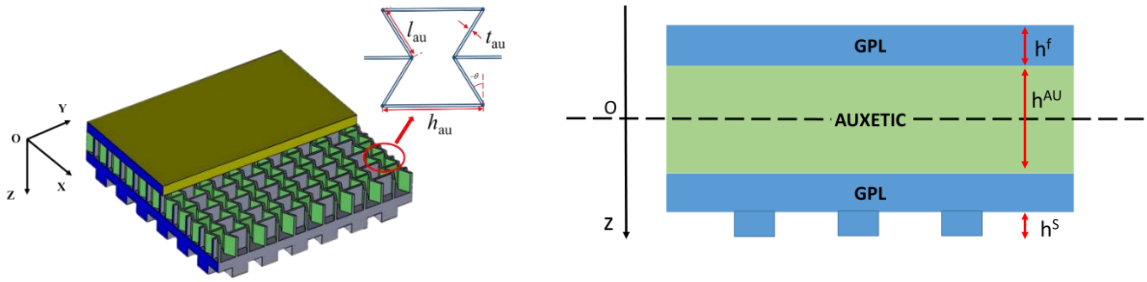

Figure 1. Eccentrically stiffened sandwich plates with auxetic honeycomb core model.

h^f The thickness of face sheets h_{au} The length of vertical cell l_{au} The length of inclined cell

h^{AU} The thickness of auxetic core h^{S} The thickness of stiffeners t_{au} The thickness of cell wall

Graphene platelet –reinforced composite face sheets

The functions of non – dimensional thickness coordinate:

$$Q_{11}^{GRA}=Q_{22}^{GRA}=E^{GRA}/\left[1-\left(\nu_{12}^{GRA}\right)^2\right],Q_{12}^{GRA}=\nu_{12}^{GRA}Q_{22}^{GRA},Q_{66}^{GRA}=G_{12}^{GRA},Q_{44}^{GRA}=G_{23}^{GRA},Q_{55}^{GRA}=G_{13}^{GRA}. \quad (2)$$

in which, the Halpin - Tsai model is selected to calculate the elastic modulus of the GPL layer. The material properties E,α,ν,ρ are the Young's modulus, the thermal expansion, the Poisson coefficient and the mass density, respectively. The symbol with '$_{GPL}$' and '$_{m}$' represent graphene material and matrix, respectively. V - the volume fractions, a_{GPL},b_{GPL},h_{GPL} - the average length, width and thickness graphene.

$$E^{GRA}=E_m/8/\left(1-\eta_L V_{GPL}\right)\left[3\eta_L\left(1/\eta_L+2a_{GPL}V_{GPL}/h_{GPL}\right)+5\eta_T\left(1/\eta_L+2b_{GPL}V_{GPL}/h_{GPL}\right)\right],$$
$$\eta_L=h_{GPL}\left(E_{GPL}-E_m\right)/\left(E_{GPL}h_{GPL}+E_m 2a_{GPL}\right),\quad \eta_T=h_{GPL}\left(E_{GPL}-E_m\right)/\left(E_{GPL}h_{GPL}+2b_{GPL}E_m\right). \quad (3)$$

The mass density and Poisson's ratio of the GPL layer are calculated by applying the rule of mixture as follows [12]:

$$\nu_{12}^{GRA}=\nu_{21}^{GRA}=V_m\left(\nu_m-\nu_{GPL}\right)+\nu_{GPL},\ V_{GPL}=1-V_m,$$
$$\alpha_1^{GRA}=\alpha_2^{GRA}=\left(V_{GPL}E_{GPL}\alpha_{GPL}+E_m\alpha_m-V_{GPL}E_m\alpha_m\right)/\left(V_{GPL}E_{GPL}+E_m-V_{GPL}E_m\right). \quad (4)$$

Auxetic honeycomb core

The functions of non – dimensional thickness coordinate and elastic modulus of the auxetic layer are calculated by [13,14]

$$Q_{11}^{AU}=E_m n_3^3\left(\eta_1-\sin\theta\right)/\left[\cos^3\theta\left[1+\left(\tan^2\theta+\eta_1\sec^2\theta\right)\eta_3^2\right]\left(1-\nu_{12}^{AU}\nu_{21}^{AU}\right)\right];$$
$$Q_{22}^{AU}=E_m n_3^3/\left[\cos\theta\left(\eta_1-\sin\theta\right)\left(\tan^2\theta+\eta_3^2\right)\left(1-\nu_{12}^{AU}\nu_{21}^{AU}\right)\right];Q_{12}^{AU}=\nu_{12}^{AU}Q_{22}^{AU},Q_{44}^{AU}=G_m\eta_3\cos\theta/\left(\eta_1-\sin\theta\right);$$
$$Q_{55}^{AU}=\frac{G_m\eta_3}{2\cos\theta}\left[\frac{\eta_1-\sin\theta}{1+2\eta_1}+\frac{\eta_1+2\sin^2\theta}{2\left(\eta_1-\sin\theta\right)}\right],\ \nu_{12}^{AU}=\frac{-\sin\theta\left(1-n_3^2\right)\left(\eta_1-\sin\theta\right)}{\cos^2\theta\left[1+\left(\tan^2\theta+\sec^2\theta\eta_1\right)\eta_3^2\right]};$$
$$Q_{66}^{AU}=E_m\eta_3^3/\left[\eta_1\left(1+2\eta_1\right)\cos\theta\right];\nu_{21}^{AU}=-\sin\theta\left(1-\eta_3^2\right)/\left(\tan^2\theta+\eta_3^2\right)/\left(\eta_1-\sin\theta\right). \quad (5)$$
$$\rho^{AU}=\frac{t_{au}\rho_m\left(h_{au}+2l_{au}\right)}{2l_{au}\cos\theta\left(h_{au}-l_{au}\sin\theta\right)};\ \alpha_1^{AU}=\alpha_m\frac{\eta_3\cos\theta}{\sin\theta+\eta_1};\ \alpha_2^{AU}=\alpha_m\frac{t_{au}\left(h_{au}+l_{au}\sin\theta\right)}{l_{au}\left(2h_{au}+l_{au}\right)\cos\theta}.$$

2.2 Problem solving

In this reseach, the basic equations are established according to FSDT. The strain-displacement relations and the stress-strain relations with the effect of thermal environment are defined as [11]

The stress component for stiffener is described by the formula [10]:

$$\begin{bmatrix}\sigma_x^S\\ \sigma_y^S\end{bmatrix}=E^S\begin{bmatrix}\varepsilon_x\\ \varepsilon_y\end{bmatrix}-\frac{E^S}{1-2\nu^S}\alpha^S\Delta T. \quad (6)$$

The force and moment resultants of eccentrically stiffened sandwich plates with auxetic honeycomb core and GPL-RC face layers are expressed as

$$\begin{aligned}&\left(N_i, M_i\right)=2\left(N_i^{GRA}, M_i^{GRA}\right)+\left(N_i^{AU}, M_i^{AU}\right)+\left(N_i^{S}, M_i^{S}\right),\ i=x,y,xy,\\&\left(Q_i\right)=2\left(Q_i^{GRA}\right)+\left(Q_i^{AU}\right),\ i=x,y,\end{aligned} \tag{7}$$

The $A_{ij}, \Phi_1, \Phi_2, \Phi_3, \Phi_{4,} I_0, I_1, I_2$ coefficients are obtained after calculating the Eq.(7)

Expression of blast loads are shown below

$$P_s = 1.8P_{sMax}\ 1-t/T_s\ \ e^{-b_s t/T_s}\ \mathrm{s} \tag{8}$$

The geometrical compatibility equation for an imperfect plate is written as [10]

$$\frac{\partial^2\varepsilon_x^0}{\partial y^2}+\frac{\partial^2\varepsilon_y^0}{\partial x^2}-\frac{\partial^2\gamma_{xy}^0}{\partial x\partial y}=\left(\frac{\partial^2 w}{\partial x\partial y}\right)^2-\frac{\partial^2 w}{\partial x^2}\frac{\partial^2 w}{\partial y^2}+2\frac{\partial^2 w}{\partial x\partial y}\frac{\partial^2 w^*}{\partial x\partial y}-\frac{\partial^2 w}{\partial x^2}\frac{\partial^2 w^*}{\partial y^2}-\frac{\partial^2 w}{\partial y^2}\frac{\partial^2 w^*}{\partial x^2} \tag{9}$$

According to FSDT, the motion equations of the sandwich plates on elastic foundation are written

$$N_{x,x}+N_{xy,y}=I_0u_{0,tt}+I_1\phi_{x,tt} \tag{10a}$$

$$N_{xy,x}+N_{y,y}=I_0v_{0,tt}+I_1\phi_{y,tt} \tag{10b}$$

$$\begin{aligned}&Q_{x,x}+Q_{y,y}+N_x\left(\mathrm{w}_{0,xx}+\mathrm{w}^*_{,xx}\right)+2N_{xy}\left(\mathrm{w}_{0,xy}+\mathrm{w}^*_{,xy}\right)+N_y\left(\mathrm{w}_{0,yy}+\mathrm{w}^*_{,yy}\right)\\&-K_1\mathrm{w}_0+K_2\left(\mathrm{w}_{0,xx}+\mathrm{w}_{0,yy}\right)+q=I_0\mathrm{w}_{0,tt}\end{aligned} \tag{10c}$$

$$M_{x,x}+M_{xy,y}-Q_x=I_2\phi_{x,tt}+I_1u_{0,tt} \tag{10d}$$

$$M_{xy,x}+M_{y,y}-Q_y=I_2\phi_{y,tt}+I_1v_{0,tt} \tag{10e}$$

The Airy's stress function $f\left(x,y,t\right)$ is introduced to simplify the problem as [12].

$$N_x=f_{,yy}, N_y=f_{,xx}, N_x=f_{,xy}, \tag{11}$$

Two cases of boundary conditions are carried out in this study.

Case 1: The imperfect plate edges are simply supported and freely movable (FM);

Case 2: The imperfect plate edges are simply supported and immovable (IM).

The analytical solutions are assumed to have the form as [12]

$$\begin{aligned}&w\left(x,y,t\right)=W\left(t\right)\sin\left(\alpha x\right)\sin\left(\beta y\right);\\&\phi_x\left(x,y,t\right)=\Phi_x\left(t\right)\cos\left(\alpha x\right)\sin\left(\beta y\right);\\&\phi_y\left(x,y,t\right)=\Phi_y\left(t\right)\sin\left(\alpha x\right)\cos\left(\beta y\right),\end{aligned} \tag{12}$$

For initial imperfection, assume that the function w^* has the same form

$$w^*\left(x,y,t\right)=\mu h\sin\left(\alpha x\right)\sin\left(\beta y\right),$$

Where $\alpha=m\pi/a, \beta=n\pi/b$, and $W(t), \Phi_x, \Phi_y$ - the amplitudes which are functions dependent on time. μ $(0\le\mu\le1)$ is a quantity that is characteristic of the structural imperfection.

The form of stress function is obtained as

$$f(x,y,t)=\mathrm{T}_1(t)\cos(2\alpha x)+\mathrm{T}_2(t)\cos(2\beta y)+\mathrm{T}_3(t)\sin(\alpha x)\sin(\beta y)+N_{x0}y^2/2+N_{y0}x^2/2 \quad (13)$$

$$\mathrm{T}_1=-\left(W^2+2W\mu h\right)\left(\Delta\beta^2/32A_{11}\alpha^2\right),\mathrm{T}_2=-\left(W^2+2W\mu h\right)\left(\Delta\alpha^2/32A_{22}\beta^2\right),\ \mathrm{T}_3=D_1\Phi_x+D_2\Phi_y,$$

Where $\Delta=A_{12}A_{21}-A_{22}A_{11}$,

$$D_1=\left[\left(\frac{\left(A_{22}A_{13}-A_{12}A_{23}\right)}{\Delta}+\frac{A_{32}}{A_{31}}\right)\alpha\beta^2+\frac{\left(A_{11}A_{23}-A_{21}A_{13}\right)}{\Delta}\alpha^3\right]/\left[\frac{A_{11}}{\Delta}\alpha^4+\frac{A_{22}}{\Delta}\beta^4-\left(\frac{A_{12}}{\Delta}+\frac{A_{21}}{\Delta}+\frac{1}{A_{31}}\right)\alpha^2\beta^2\right];$$

$$D_2=\left[\left(\frac{\left(A_{11}A_{24}-A_{21}A_{14}\right)}{\Delta}+\frac{A_{32}}{A_{31}}\right)\beta\alpha^2+\frac{\left(A_{22}A_{14}-A_{12}A_{24}\right)}{\Delta}\beta^3\right]/\left[\frac{A_{11}}{\Delta}\alpha^4+\frac{A_{22}}{\Delta}\beta^4-\left(\frac{A_{12}}{\Delta}+\frac{A_{21}}{\Delta}+\frac{1}{A_{31}}\right)\alpha^2\beta^2\right].$$

Through transformations, and by applying the Bubnov - Galerkin method, the new equations for the imperfect plate are rewritten as follows:

$$\begin{aligned}
&h_{11}\mathrm{W}+h_{12}\Phi_x+h_{13}\Phi_y+h_{14}\left(\mathrm{W}+\mu h\right)\Phi_x+h_{15}\left(\mathrm{W}+\mu h\right)\Phi_y+h_{16}\left(\mathrm{W}+\mu h\right),\\
&\quad+h_{17}W\left(\mathrm{W}+\mu h\right)\left(W+2\mu h\right)+F\left(\mathrm{W}+\mu h\right)+h_{18}q=I_0W_{,tt},\\
&h_{21}\Phi_x+h_{22}\Phi_y+h_{23}\left(\mathrm{W}+\mu h\right)+h_{24}W\left(W+2\mu h\right)=\left[I_2-\left(I_1^2/I_0\right)\right]\Phi_{x,tt},\\
&h_{31}\Phi_x+h_{32}\Phi_y+h_{33}\left(\mathrm{W}+\mu h\right)+h_{34}W\left(W+2\mu h\right)=\left(I_2-\left(I_1^2/I_0\right)\right)\Phi_{y,tt}.
\end{aligned} \quad (14)$$

With h_{ij} are given in Appendix.

Nonlinear dynamic analysis with effect of pre-loaded axial compression

Assume that the plate is loaded under uniform compressive loads P_x and P_y (Pascal) on the edges $x=(0,a)$ and $y=(0,b)$ (FM case) with: $N_{x0}=-P_xh,\ N_{y0}=-P_yh.$

Nonlinear dynamic analysis in thermal environment

The effect of temperature on the structure will be considered in case 2 (IM), corresponding to the condition: the plate with all edges which are simply supported and immovable. Under the influence of thermal load, the condition expressing the immovability on the edges is satisfied in an average sense as

$$\int_0^b\int_0^a\frac{\partial u}{\partial x}dxdy=0,\ \int_0^a\int_0^b\frac{\partial v}{\partial y}dxdy=0. \quad (15)$$

In accordance with this average sense, the respective force components are calculated as follows:

$$\begin{aligned}
N_{x0}&=c_{11}\Phi_x+c_{12}\Phi_y+c_{14}\mathrm{W}^2+c_{15}\mathrm{W}\mu h+\Phi_1,\\
N_{y0}&=c_{21}\Phi_x+c_{22}\Phi_y+c_{24}\mathrm{W}^2+c_{25}\mathrm{W}\mu h+\Phi_2.
\end{aligned} \quad (16)$$

With c_{ij} coefficients obtained after calculating the Eq.(16).

3. Results and Discussion

To evaluate the reliability of the calculation, we compare the natural frequency values of the isotropic plate. The natural frequency of the first mode and second mode are shown in Table 1. The natural frequency values of the two modes in this study are very close to the results of the solutions of Hashemi et al. [15,16]. It can be seen that the obtained results in this study are very reliable.

Table 1. Comparison study of natural frequency $\beta = \left(\omega a^2/h\right)\sqrt{\rho_c/E_c}$ for isotropic plate.

Material		First mode			Second mode		
		h/a			h/a		
		0.05	0.1	0.2	0.05	0.1	0.2
Fully ceramic	Present	5.9317	5.8117	5.3957	14.677	13.98	11.941
	[15]	0.177%	0.639%	1.859%	0.417%	1.348%	2.807%
	[16]	0.174%	0.634%	1.856%	0.417%	1.341%	2.798%
Fully metallic	Present	3.0192	2.9581	2.7463	7.4704	7.1158	6.0778
	[15]	-0.45%	0.02%	1.28%	-0.21%	0.76%	2.29%
	[16]	0.18%	0.64%	1.85%	0.41%	1.35%	2.80%

Geometrical parameters of eccentrically stiffened sandwich plates with auxetic honeycomb core and GPL-RC face layers selected for the investigation are as follows: $a/b=1, a/h=25, h^{AU}=0.5h$, $h^f=h^s=0.5h^{AU}$, $b_1=b_2=h^s, d_1=d_2=2h^s$. Material parameters used to investigate are as follows: $V_{GPL}=0.11, E_{GPL}=1010GPa, E_m=69GPa, \nu_{GPL}=0.186, \nu_m=0.33, \alpha_{GPL}=5\times10^{-6}K^{-1}, \alpha_m=23\times10^{-6}K^{-1}$, $\rho_{GPL}=1062.5kg/m^3, \rho_m=2700kg/m^3$. Geometrical parameters of graphene platelets used to investigate are as follows: $t_{GPL}=1.5nm, w_{GPL}=1.5\mu m, l_{GPL}=2.5\mu m$.

The results below evaluate the influence of elastic foundation, geometrical parameters, material parameters, load and temperature environment on the dynamic response and natural frequency of eccentrically stiffened sandwich plates with auxetic honeycomb core and GPL-RC face layers under blast loading. Figures 2 and 3 demonstrate the impact of the geometric parameters on the behavior of eccentrically stiffened sandwich plates with auxetic honeycomb core and GPL-RC face layers under blast loading. In Figure 2, we keep parameter a and change estimation of parameter b. It can be seen that the amplitude of the dynamic response decreases when the proportion *a/b* rises . It is obvious from Figure 3 that the plates have critical change when the length to thickness proportion of the plate changes, and that the ratio *a/h* increases leads to reduction in the capacity of plates.

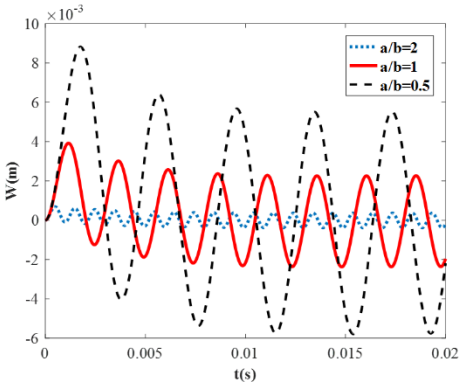

Figure 2. Influence of ratio *a/b*

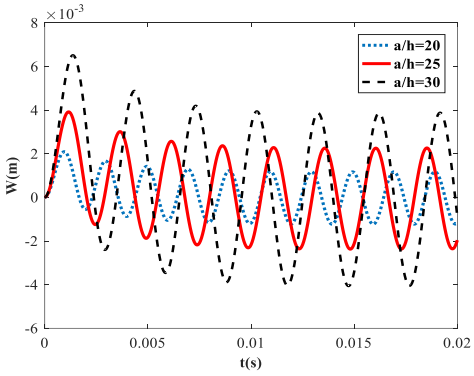

Figure 3. Influence of ratio *a/h*

Figures 4 demonstrates the impact of GPL volume fraction on the behavior of the plate. GPL causes the amplitude of the deformation-time curve of the plate to decrease. The amplitude of the deformation-time curve increases when the imperfection coefficient increases. Figures 5 demonstrates the impact of

the Winkler and Pasternak foundation on the dynamic response of the plate. From figure 5 we can see that the modulus of the elastic base has a positive effect on the nonlinear dynamic response. On the other hand, it is clearly seen that Pasternak foundation has bigger impact on nonlinear dynamic response than Winkler foundation. The stiffeners make the plate more resistant, which is shown in Figure 6. Table 2 shows that the stiffeners and the foundation also increase the natural frequency of eccentrically stiffened sandwich plates with auxetic honeycomb core and GPL-RC face layers. Figure 7 shows that the temperature environment has an adverse effect on the performance of the structure. Figures 8 and 9 show the influence of amplitude of blast load and compression load on the dynamic response of the sandwich plates. Apparently, the amplitude of blast load (P_s) and compression load (P_x) decrease, which leads to reduction in the amplitude of the dynamic response of the sandwich plates.

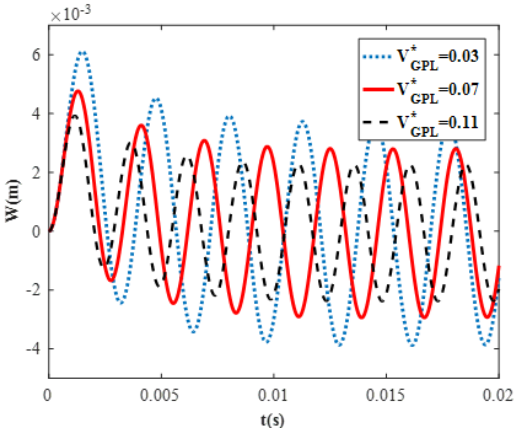

Figure 4. Influence of GPL volume fraction.

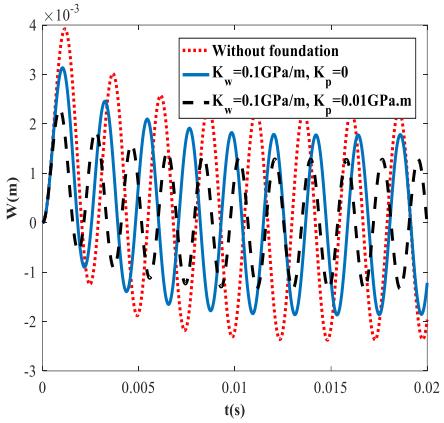

Figure 5. Influence of foundation.

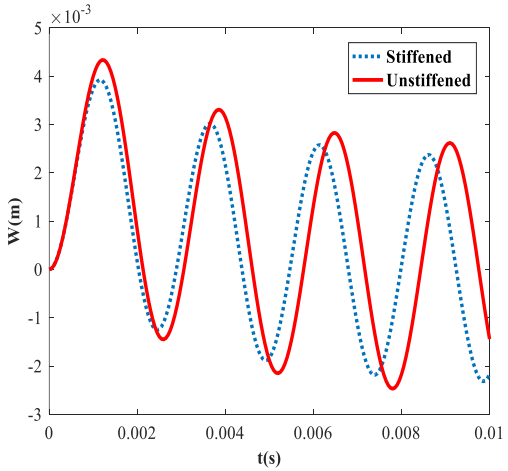

Figure 6. Influence of stiffeners.

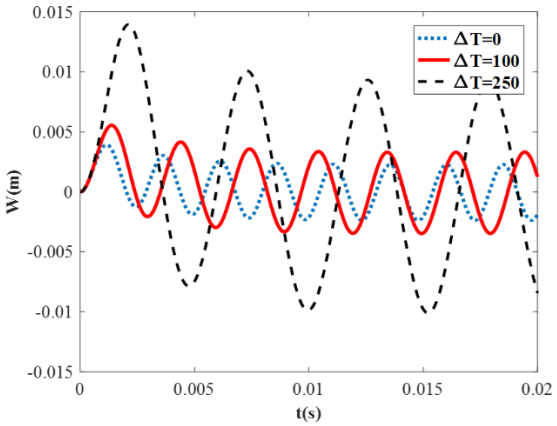

Figure 7. Influence of temperature.

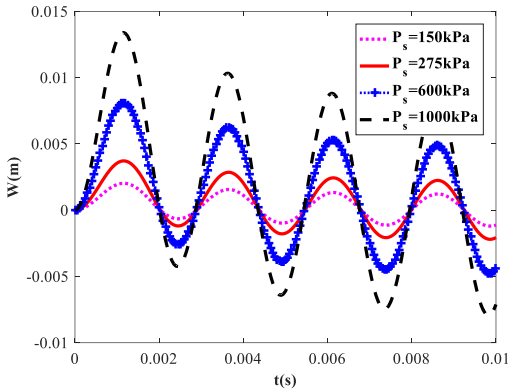

Figure 8. Influence of blast load.

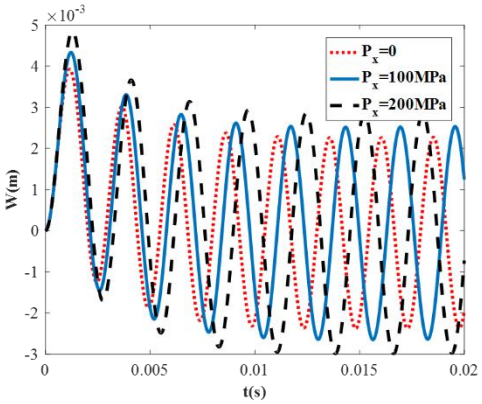

Figure 9. Influence of compression load.

Table 2. Effect of pre-loaded, foundation and stiffeners on natural frequencies $\beta_{om} = \omega \times h \times \sqrt{\rho_m / E_m} / a^2$.

Foundation	**Mode**	$P_x(MPa)$				
		0	100	200	300	500
$K_w = 0$	Stiffened	0.0192	0.0181	0.0171	0.0159	0.0133
$K_p = 0$	Unstiffened	0.0181	0.0171	0.0159	0.0147	0.0118
$K_w = 0.1GPa/m$	Stiffened	0.0216	0.0207	0.0198	0.0188	0.0167
$K_p = 0$	Unstiffened	0.0207	0.0198	0.0188	0.0178	0.0155
$K_w = 0.2GPa/m$	Stiffened	0.0334	0.0328	0.0322	0.0316	0.0304
$K_p = 0.03GPa.m$	Unstiffened	0.0328	0.0322	0.0316	0.0310	0.0297

4. Conclusion

This paper investigated the nonlinear dynamic response of eccentrically stiffened sandwich thick plates with auxetic honeycomb core and GPL-RC face layers under blast loading on elastic foundation based on the first order shear deformation theory and Airy stress function. The numerical results for the dynamic response of the plates were obtained by Runge-Kutta method. More specifically, in the study,

•The natural frequency results were compared with other studies;

• The foundation and stiffeners had positive impact on time-amplitude response curves of the plates;

• The temperature field had significant impact on the nonlinear dynamic response of eccentrically stiffened sandwich plates with auxetic honeycomb core and GPL-RC face layers. In addition, the temperature increment had negative effect on the amplitudes of the plates; and

• The shape parameter, imperfection coefficient, and external loads were considered.

Acknowledgments

This work was partly supported by VNU University of Engineering and Technology under Project CN20.04

References

[1] N. V. Nguyen, N. X. Hung, T. N. Nguyen, J. Kang, J. Lee, A Comprehensive Analysis of Auxetic Honeycomb Sandwich Plates with Graphene Nanoplatelets Reinforcement, Compos. Struct, Vol. 259, 2021, 113213, https://doi.org/10.1016/j.compstruct.2020.113213.

[2] C. Li, H. S. Shen, H. Wang, Postbuckling Behavior of Sandwich Plates With Functionally Graded Auxetic 3D Lattice Core, Compos. Struct, Vol. 237, 2020, 111894, https://doi.org/10.1016/j.compstruct.2020.111894.

[3] C. Li, H. S. Shen, H. Wang, Z. Yu, Large Amplitude Vibration of Sandwich Plates With Functionally Graded Auxetic 3D Lattice Core, Int. J. Mech. Sci, Vol. 174, 2020, 105472, https://doi.org/10.1016/j.ijmecsci.2020.105472.

[4] M. H. Hajmohammad, R. Kolahchi, M. S. Zarei, A. H. Nouri, Dynamic Response of Auxetic Honeycomb Plates Integrated with Agglomerated CNT-Reinforced Face Sheets Subjected to Blast Load Based on Visco-Sinusoidal Theory, Int. J. Mech. Sci, Vol. 153–154, 2019, pp. 391–401, https://doi.org/10.1016/j.ijmecsci.2019.02.008.

[5] J. Zhang, X. Zhu, X. Yang, W. Zhang, Transient Nonlinear Responses of An Auxetic Honeycomb Sandwich Plate Under Impact Loads, Int. J. Impact Eng, Vol. 134, 2019, 103383, https://doi.org/10.1016/j.ijimpeng.2019.103383.

[6] N. D. Duc, P. H. Cong, Nonlinear Dynamic Response and Vibration of Sandwich Composite Plates with Negative Poisson's Ratio in Auxetic Honeycombs, J. Sandw. Struct. Mater, Vol. 20, 2016, pp. 692–717, https://doi.org/10.1177/1099636216674729.

[7] H. T. Thai, T. K. Nguyen, T. P. Vo, J. Lee, Analysis of Functionally Graded Sandwich Plates Using A New First-Order Shear Deformation Theory, Eur. J. Mech. A/Solids, Vol. 45, 2014, pp. 211–225, https://doi.org/10.1016/j.euromechsol.2013.12.008.

[8] N. T. Phuong, V. H. Nam, D. T. Dong, Nonlinear Vibration of Functionally Graded Sandwich Shallow Spherical Caps Resting on Elastic Foundations by Using First-Order Shear Deformation Theory in Thermal Environment, J. Sandw. Struct. Mater, Vol. 22, 2018, pp. 1157–1183, https://doi:10.1177/1099636218782645.

[9] S. Amir, M. Khorasani, H. BabaAkbar-Zarei, Buckling Analysis of Nanocomposite Sandwich Plates with Piezoelectric Face Sheets Based on Flexoelectricity and First-Order Shear Deformation Theory, J. Sandw. Struct. Mater, Vol. 22, 2018, pp. 2186–2209, https://doi:10.1177/1099636218795385.

[10] N. D. Duc, P. H. Cong, V. D. Quang, Nonlinear Dynamic and Vibration Analysis of Piezoelectric Eccentrically Stiffened FGM Plates in Thermal Environment, Int. J. Mech. Sci, Vol. 115–116, 2016, pp. 711–722, https://doi.org/10.1016/j.ijmecsci.2016.07.010.

[11] N. D. Duc, V. D. Quang, P. D. Nguyen, T. M. Chien, Nonlinear Dynamic Response of Functional Graded Porous Plates on Elastic Foundation Subjected to Thermal and Mechanical Loads, J. Appl. Comput. Mech, Vol. 4, No. 4, 2018, pp. 245–259, https://dx.doi.org/10.22055/jacm.2018.23219.1151.

[12] N. D. Duc, Nonlinear Static and Dynamic Stability of Functionally Graded Plates and Shells, Vietnam Natl Univ Press, Hanoi, 2014.

[13] P. H. Cong, P. K. Quyet, N. D. Duc, Effects of Lattice Stiffeners and Blast Load on Nonlinear Dynamic Response and Vibration of Auxetic Honeycomb Plates, Proc. Inst. Mech. Eng. C: J. Mech. Eng. Sci, 2021, https://doi.org/10.1177/0954406221992797

[14] N. D. Duc, T. Q. Quan, P. H. Cong, Nonlinear Vibration of Auxetic Plates and Shells, Vietnam Natl Univ Press, Hanoi, 2021.

[15] S. H. Hashemi, M. Fadaee, S. R. Atashipour, A New Exact Analytical Approach for Free Vibration of Reissner–Mindlin Functionally Graded Rectangular Plates, Int. J. Mech. Sci, Vol. 53, 2011, pp. 11–22, https://doi.org/10.1016/j.ijmecsci.2010.10.002.

[16] S. H. Hashemi, M. Arsanjani, Exact Characteristic Equations for Some of Classical Boundary Conditions of Vibrating Moderately Thick Rectangular Plates, Int. J. Solids Struct, Vol. 42, No. 3–4, 2005, pp. 819–853, https://doi.org/10.1016/j.ijsolstr.2004.06.063.

Appendix

$h_{11} = -K_W - K_P\left(\alpha^2 + \beta^2\right), h_{12} = -A_{61}\alpha,\ h_{13} = -A_{71}\beta, h_{14} = 32\alpha\beta/(3ab)D_1,\ l_{15} = 32\alpha\beta/(3ab)D_2,$

$h_{16} = -\left(A_{61}\alpha^2 + A_{71}\beta^2\right), h_{17} = \alpha^4\Delta/(16A_{22}) + \beta^4\Delta/(16A_{11}),\ h_{18} = 16/(\alpha\beta ab), F = \left(-N_{x0}\alpha^2 - N_{y0}\beta^2\right),$

$h_{21} = -\left(A_{13}\left(A_{22}A_{13} - A_{12}A_{23}\right)/\Delta + A_{23}\left(A_{11}A_{23} - A_{21}A_{13}\right)/\Delta + A_{43}\right)\alpha^2 - D_1\left(A_{13}A_{12}/\Delta - A_{23}A_{11}/\Delta\right)\alpha^3 - A_{61}$

$-D_1\left(A_{23}A_{21}/\Delta - A_{13}A_{22}/\Delta - A_{32}/A_{31}\right)\alpha\beta^2 - \left(A_{52} - A_{32}^2/A_{31}\right)\beta^2, h_{24} = -8\beta\left[A_{13}A_{12} - A_{23}A_{11}\right]/(3abA_{11}),$

$h_{22} = -\left(A_{13}\left(A_{22}A_{14} - A_{12}A_{24}\right)/\Delta + A_{23}\left(A_{11}A_{24} - A_{21}A_{14}\right)/\Delta + A_{44} + A_{52} - A_{32}^2/A_{31}\right)\beta\alpha$

$-D_2\left(A_{13}A_{12}/\Delta - A_{23}A_{11}/\Delta\right)\alpha^3 - D_2\left(A_{23}A_{21}/\Delta - A_{13}A_{22}/\Delta - A_{32}/A_{31}\right)\alpha\beta^2, h_{23} = -A_{61}\alpha.$

$h_{32} = -\left(A_{23}\left(A_{22}A_{14} - A_{12}A_{24}\right)/\Delta + A_{24}\left(A_{11}A_{24} - A_{21}A_{14}\right)/\Delta + A_{45}\right)\beta^2 - D_2\left(A_{24}A_{21}/\Delta - A_{23}A_{22}/\Delta\right)\beta^3 - A_{71}$

$-D_2\left(A_{23}A_{12}/\Delta - A_{24}A_{11}/\Delta - A_{32}/A_{31}\right)\alpha^2\beta - \left(A_{52} - A_{32}^2/A_{31}\right)\beta^2, h_{34} = -8\alpha\left[A_{24}A_{21} - A_{23}A_{22}\right]/(3abA_{22}),$

$h_{31} = -\left(A_{23}\left(A_{22}A_{13} - A_{12}A_{23}\right)/\Delta + A_{24}\left(A_{11}A_{23} - A_{21}A_{13}\right)/\Delta + A_{44} + A_{52} - A_{32}^2/A_{31}\right)\beta\alpha$

$-D_1\left(A_{24}A_{21}/\Delta - A_{23}A_{22}/\Delta\right)\beta^3 - D_1\left(A_{23}A_{12}/\Delta - A_{24}A_{11}/\Delta - A_{32}/A_{31}\right)\alpha^2\beta, h_{23} = -A_{71}\beta.$